Dynamic Analysis of Human Movement: Gait and Mountain Climber

Ana Lopes (98587)[1], Daniel Galhoz (90791)[2], Mariana Mourão (98473)[3] and Rita Almeida (90180)[4]

[1] *Instituto Superior Técnico,*
Integrated Master's in Biomedical Engineering,
ana.rita.santos.lopes@tecnico.ulisboa.pt

[2] *Instituto Superior Técnico,*
Integrated Master's in Biomedical Engineering,
daniel.galhoz@tecnico.ulisboa.pt

[3] *Instituto Superior Técnico,*
Integrated Master's in Biomedical Engineering,
mariana.mourao@tecnico.ulisboa.pt

[4] *Instituto Superior Técnico,*
Integrated Master's in Biomedical Engineering,
rita.margarida.almeida@tecnico.ulisboa.pt

ABSTRACT — *The dynamic analysis of human motion provides a more in-depth study of human motion. Hence, the main goal of the present work was the continuing of the analyze done in the first part of the project, regarding the kinematic analysis, by studying the dynamic analysis of the two movements in the sagittal plane - gait cycle and the mountain climber exercise, in a multibody biomechanical system, considering the data acquired in the Biomechanics of Motion Laboratory at Instituto Superior Técnico, as well as the 2D Multibody Model defined with MATLAB. For both movements it was analyzed electromyography (EMG) activity data, ground reaction force and the center of pressure collected, with the former being recorded by four electrodes placed on leg muscles (Gastrocnemius Medialis, Tibialis Anterior, Rectus Femoris and Biceps Femoris), and the last two by 3 force plates positioned on the floor, which the volunteer had to walk. Regarding the gait movement, it was compared the results obtained for the acquired data with the ones from Winter [1], considering data related to the performance of a slow cadence gait (information taken from the previous work) whereas for the mountain climber exercise, this comparison was not possible as studies concerning this movement are scarce. The results for the gait movement showed similar curve´s shapes from those found in the literature, when considering the variability across subjects. The results concerning the mountain climber exercise were all within what was expected for this movement. With the results obtained being similar to the ones found in literature, at least regarding the gait movement, it can be assumed that the mathematical model implemented shows coherent results that allowed a detailed analysis of the movements.*

1 Introduction

A dynamic analysis is crucial for an in-depth study of movement, as it involves both kinematic and kinetic data. In other words, this type of analysis concerns a biomechanical study of what can be observed visually when watching a body in motion and the forces associated with said motion. The forces to be considered involve the individual muscle forces, the moments generated by those muscles across a joint, the mechanical power patterns, or energy patterns.[1] [2]

In the first part of this project, a kinematic analysis was performed on the two chosen motions: the gait and the mountain climber exercise.[3] For this paper, the main focus will be the study of the forward dynamics regarding the same motions, where, through a mathematical model, it is possible to describe how coordinates and their velocities change due to applied forces and moments. This can be achieved by solving the dynamic equilibrium equations of each rigid body - all the acting forces result in equal and oppositely directed inertial forces - in the multi-body system implemented.

2 Methodology

2.1 Experimental Data Acquisition

Besides the kinematic data acquisition more extensively covered in part I [3], for the kinetic data acquisition three force plates, positioned below the subject's path, were used, allowing to collect the three components of the ground reaction forces (GRFs) and the trajectory of the center of pressure (CoP). Regarding this acquisition, for the second movement the subject stood on two of the force plates, with the hands being on the third plate and the foots on the first. Thus, regarding these movement, only these force plates will be processed and analyzed.

Additionally, muscle activity was recorded with an electromyograph (EMG), by placing four electrodes on right leg muscles (Gastrocnemius Medialis, Tibialis Anterior, Rectus Femoris and Biceps Femoris), being synchronized with the motion capture system. The root-mean-square (RMS) envelopes of the EMG signals were provided besides the raw data.

2.2 Pre-processing

The formulation of the multibody model system follows what was defined in part I [3] of this project, being its description extended to the mass ratio (normalized by the subject's weight) and radius of gyration ratio (normalized by the segment length, with respect to the center of mass) of the 14 bodies, defined from anthropometric data. Regarding the GRFs, for each of the force plates it was defined the bodies on which the force could be applied (foot or phalanges), providing the respective normalized (by the segment length) local coordinates. The text file structure of the biomechanical model is specified in Appendix A, being its values read and stored by the function *ReadProcessingFile.m*.

Posteriorly, the projection of the 3D spatial coordinates raw data onto the 2D sagittal plane is performed by the function *ReadProcessData.m*, according to the definition of the biomechanical model, being the data filtered by a fourth-order zero-lag Butterworth low-pass digital filter (function *FilterCoordinates.m*), with the selection of the cut-off frequency achieved through a residual analysis. Appendix B displays the cut-off frequencies for each of the bodies, regarding both movements performed, which was obtained by the function *bargraphCutOffFrequencies.m*.

Next, the body segments' length was computed from the static data by applying the function *ComputeAverageLength.m*, corresponding to an average length over all time frames, being the length in each time frame computed as the distance between the two edge points of the body. This allows to update the previously normalized anthropometry data, regarding the positions and angles (function *EvaluatePositions.m*, applied for the dynamic movements), and moment of inertia (function *ComputeBodyProperties.m*) for all bodies. The function

ComputeBodyProperties.m also estimates the mass m by multiplying the total body mass (69 kg) by the previously stored mass ratio, while the moment of inertia J was computed by Equation (2.1).

$$J_i = m_i \times (R_i \times L_i)^2 \tag{2.1}$$

As for the preprocessing of the force plate data, the function *ReadGRF.m* was applied. The components x and z of the GRFs were filtered with a low-pass Butterworth, with the optimal cut-off frequency selected through a residual analysis. Since the force plates record a residual force (~1-4 N) when there is no contact, the forces were set to 0 N when the vertical component of the GRF was below 7 N, being the filtered process repeated. For the position of the CoPs, components x and z (CoPx and CoPz) were filtered with a fixed frequency of 10Hz. Once again, when there is no contact on the force plate, it immediately resets the CoP to its origin, giving rise to a discontinuity in its the representation. To improve the filtering procedure, the frames in which no contact existed were assigned the values of the closest known contact points. Appendix C displays a graphical comparison between filtration procedures of GRF and CoP data.

Finally, the function *WritesModelInput.m* organizes the data similarly to what was done for the part I of this project.[3] Data from force plates was kept with a precision of 20 digits, in order to avoid numerical inaccuracies during numerical integration.

Concerning the second movement to be studied, the acquisition data provided has more than one repetition. In order to posteriorly evaluate the variability between repetitions, the function *ComputeCycles_MC.m* computes, separately, the frames at which the right and left toes reach the floor. The data provided contains an initial period (first 26 frames) where no movement was acquired, being in a plank position. From this data it was estimated the z coordinate defining the rest state, for both right and left toes. The first frame, from consecutive frames, at which the z coordinate was below the rest state estimate were stored, which defines the start of the resting phase of the corresponding limb. This data was organized into a text file (*Cycles_MountainClimber.txt*), being its structured explained in Appendix C.

2.3 Processing

The relation between forces and motion of a constraint multibody system throughout time can be described by its equations of motion. These relate the inertial characteristics of the system with the applied external forces, $\boldsymbol{g_{ext}}$, and the internal forces generated due to the imposed kinematics restrictions, $\boldsymbol{g_{int}}$. To obtain these equations for a general multibody system, the principle of Virtual Power can be applied – Equations (2.2) and (2.3) –, which states that the virtual power of a multibody system is zero.[4]

$$P^* = f.\dot{q}^{*T} = 0 \tag{2.2}$$

$$f = M\ddot{q} - g_{ext} \tag{2.3}$$

where $\dot{q}^*$ is a vector of virtual velocities and $\boldsymbol{f}$ a vector that holds all forces that produce virtual power, including the system's inertial forces $M\ddot{q}$ and the remaining applied external forces $\boldsymbol{g_{ext}}$, being M a matrix with the overall mass of the system and $\ddot{q}$ a vector of generalized accelerations.

The virtual power produced by the internal forces that are associated with the kinematic constraints (called joint reaction forces) cancel each other, since being pairs of action and reaction forces. Given this, the internal forces $\boldsymbol{g_{int}}$ are introduced by applying the Lagrange multipliers method – Equation (2.4) –, which considers that internal forces have the direction of the constraint's violations (given by the rows of Jacobian matrix) and a magnitude given by the associate Lagrange multiplier λ.[4]

$$g_{int} = -\Phi_q{}^T \lambda \tag{2.4}$$

Because the internal forces produce a null virtual power, their virtual power can be added to equation (2.2), giving rise to the Equation (2.5).

$$P^* = \dot{q}^{*T}\left(M\ddot{q} - g_{ext} + \Phi_q{}^T\lambda\right) = 0 \Rightarrow M\ddot{q} + \Phi_q{}^T\lambda = g_{ext} \tag{2.5}$$

The system described in Equation (2.5) provides nh = 42 equations, containing only nc = 84 unknowns ($\ddot{\boldsymbol{q}}$, $\boldsymbol{\lambda}$). In order to make it a fully solvable system with one unique solution, the acceleration kinematic constraint equations are needed (Equation (2.6)), introducing the same nh number of equations and involving the same nc unknow accelerations.[4]

$$\Phi_q \ddot{q} = \gamma \tag{2.6}$$

Since the generalized position and velocity constraint equations are not explicitly used, the numerical errors inherent to the integration of the equations of motion lead to an increasing violation of the position and velocity constraints. Hence, the differential equations become unstable and the method of direct integration eventually diverges. For preventing this, the Baumgarte stabilizer was implemented, which substitutes an unstable open-loop system by a closed-loop one, in which the position and velocity constraints violations are feed-back to the acceleration constraint equations system (Equation (2.7)).[5]

$$\ddot{\Phi} + 2\alpha\dot{\Phi} + \beta^2\Phi = 0, \tag{2.7}$$

where the feedback parameters $\boldsymbol{\alpha}$ and $\boldsymbol{\beta}$ are positive constants, typically 5. Substituting $\boldsymbol{\gamma}$ by $\bar{\boldsymbol{\gamma}}$, the final formulation of the equations of motion of a multibody system for a forward dynamic analysis is given by Equation (2.8), representing an initial value problem, being solved iteratively for each time step in order of the unknown accelerations and Lagrange multipliers.

$$\begin{bmatrix} M & {\Phi_q}^T \\ \Phi_q & 0 \end{bmatrix} \begin{bmatrix} \ddot{q} \\ \lambda \end{bmatrix} = \begin{bmatrix} g_{ext} \\ \bar{\gamma} = \gamma - 2\alpha(\Phi_q \dot{q} - \nu) + \beta^2\Phi \end{bmatrix} \tag{2.8}$$

For the first time step, the initial conditions are previously corrected (function *CorrectInitialConditions.m*), by performing a position and velocity analysis with the functions *PositionAnalysis.m* (implements the Newton-Raphson method) and *VelocityAnalysis.m*, which respectively computes the position and velocity kinematic constraint equations by calling the function *Kinem_FuncEval.m*. After this, function *FuncEval.m* solves the equations of motion for each time step, returning the calculated $\ddot{q}$ and λ. From this, it is constructed a vector containing the system's velocities and accelerations ($\dot{y}_t = [\dot{q} \ \ddot{q}]^T$), which is posteriorly used to obtain the system's positions and velocities for the next time step ($y_{t+1} = [q \ \dot{q}]^T$), by performing numerical integration (function *ode45*).

To solve the equations of motion, at each time step the functions *MakeMassMatrix.m* and *MakeForceVector.m* are called to compute the system's mass matrix M (Equation (2.9)) and the external force vector g_{ext} (Equation (2.10)), respectively.

$$M_i = \begin{bmatrix} m_i & 0 & 0 \\ 0 & m_i & 0 \\ 0 & 0 & J_i \end{bmatrix}, \tag{2.9}$$

where m_i and J_i are the body's mass and moment of inertia, respectively, being the mass matrix M built by grouping the mass matrices M_i of all bodies.

$$\begin{cases} g_{i_{ext}} = \begin{bmatrix} f_{i_x} \\ f_{i_z} \\ n_i + n_{transport} \end{bmatrix} \\ n_{transport} = {s_x}^P f_x - {s_z}^P f_z \end{cases}, \tag{2.10}$$

where $g_{i_{ext}}$ is the external force vector of body i, being composed of the force f_i and the external moment n_i, with $n_{transport}$ being the transport moment that results from transferring the applied force from the point of application to the body's center of mass. The vector g_{ext} corresponds to the concatenation of all $g_{i_{ext}}$. To determine the body where each force is being applied (foot or phalanges), whenever CoPx was behind the x coordinate of the point that separates both bodies, the force was applied on the foot.

3 Results and Discussion

In this section, it is presented the results obtained through the computational implementation of the dynamic analysis regarding the performance of both movements – gait and mountain climber. Whenever possible, the results obtained are compared with the ones from the literature, as a form to assess the subject's structural and functional integrity of its biomechanical system, as well as to validate our computational implementation.

3.1 Gait movement

The kinematic analysis from the first paper concluded that the subject was performing a slow gait, namely because of being conditioned to walk over the 3 force plates positioned on the floor.[3] So, a slow cadence gait, rather than a natural one, will be considered when comparing with the literature.

3.1.1 Ground Reaction Forces

The ground reaction forces reflect the net vertical and shear forces acting on the surface of the plates, which measured them. They are an algebraic summation of the mass-acceleration products of all body segments while the foot is in contact with said platform. The vertical force reflects the accelerations due to gravity as well as the accelerations seen by the camera.[1] Figure 3.1.1 shows the averaged horizontal and vertical reaction forces, normalized to body mass (N/kg), of a slow walk from literature and of the results obtained in the laboratory session.

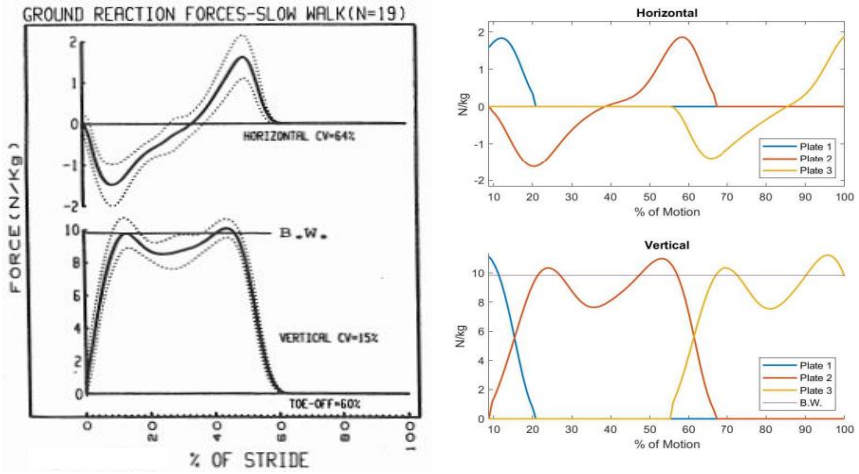

Figure 3.1.1: Horizontal (top) and vertical (bottom) Ground Reaction Forces. B.W.: Body weight. Left: Retrieved from literature.[1] Right: Results obtained with the implementation on MATLAB.

At first glance, the curves for both forces obtained from the data acquired strongly resemble the shape of those from literature. Note that, in the previous paper, it was concluded that the stance occupied 58.5% of the gait [3] and that is also corroborated in these results, as the phase ends with toe-off.

For the horizontal ground reaction force, there is an initial negative phase during the first half of stance indicating the net slowdown of the entire body, and a positive phase during the second half of stance indicating a forward acceleration of the body. The magnitude of the positive and negative peaks is related to the speed of the gait (and increases with cadence), with a 1.5 N/kg value from literature for a slow walk. The values found in the results obtained round the 1.6 and 1.8 N/kg, which are little higher than expected, but still in the acceptable interval.[1]

As for the vertical ground reaction force, there are two peaks, being that the first refers to weight-acceptance in the early stance, where there is upwards acceleration of the center of gravity, while the second corresponds to push-off in the late stance, where there is a deceleration of the center of gravity. The mean vertical force over the stance is about 9 N/kg in the literature, and the speed of the gait does not alter this mean but does reflect drastically in the amount of change in the peak-to-peak differences. Slow cadences were reported to have the least peak-to-peak differences, of 1.5 N/kg. The results obtained show a mean of 9.3 N/kg, close to the anticipated, and the differences between the maximum and minimum values round 3.4 N/kg, a variation higher than expected.[1]

3.1.2 Moment of Force

Moments of force correspond to the net result of all muscular, ligament and friction forces acting to change the angular rotation of a joint. Throughout the gait, since the extreme limits of the joint angles are not reached and the minimal friction forces are achieved, the net moment becomes a result of just muscular forces.[1] In Figure 3.1.2 are represented the results of the support, hip, knee, and ankle average joint moments of force and the net support moment (normalized for body weight (N.m/kg) and cadence) of a slow walk from the literature and the results obtained in the laboratory session.

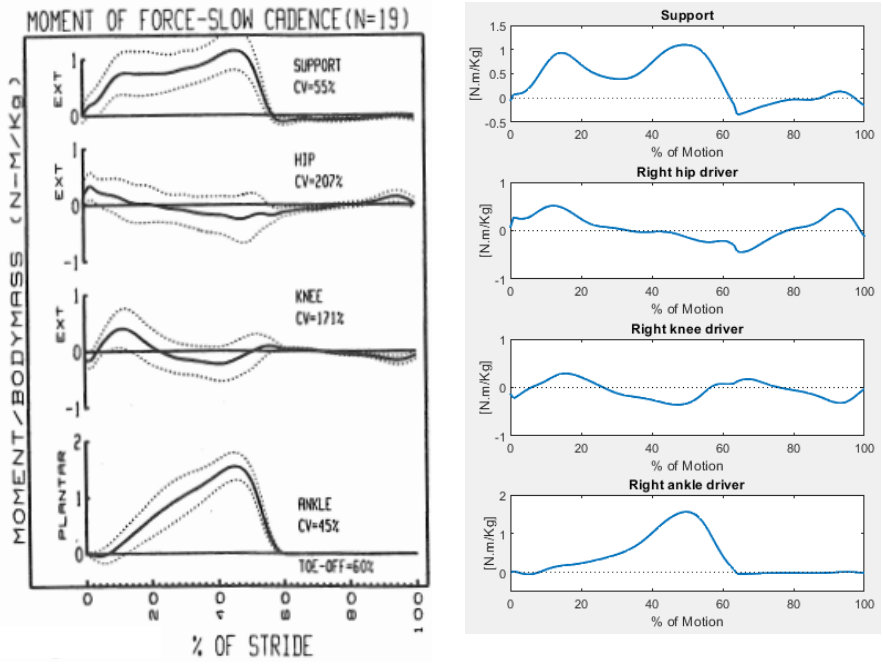

Figure 3.1.2: (From top to bottom) Moment of force for support, hip, knee, and ankle joints. Left: Retrieved from literature.[1] Right: Results obtained with the implementation on MATLAB.

Again, all the curves obtained resemble closely to the shape of those from literature, being that the only discrepancies might be related to the conditioning of consciously stepping on the force plates. The results are reported in a manner that all extensor moments are positive, as they are attempting to push the body away from the ground, and the flexor moments are considered negative, as they are attempting to bring the body downwards.[1]

As for the support moment, it is an algebraic summation of the total lower limb during stance, period during which is observed a net extensor (positive) pattern, being described by Equation (3.1).

$$M\_s = M\_a + M\_k + M\_h \tag{3.1}$$

where s, a, k, and h stand for support, ankle, knee, and hip, and M stands for the corresponding moment. While the ankle patterns are quite consistent, there is a considerable but highly correlated variability at the hip and knee, as concluded in literature. This makes the support moment pattern remain practically the same during stance

throughout trials, while the individual moments for a given subject and different strides may vary, which could be due to changes in the dominant group of muscles that supports a given joint.[1]

3.1.3 Joint Power

Mechanical power of a joint refers to the product of the joint moment of force and joint angular velocity, being described by Equation (3.3).

$$P_j = M_j \times \omega_j \,, \tag{3.2}$$

where P_j is the mechanical power of the joint, M_j is the joint moment of force and ω_j is the joint angular velocity. The muscle's role during any movement is very important, as they generate and absorb the mechanical energy necessary to accomplish said movement. This happens through the tension when they shorten and lengthen, that is, during concentric and eccentric phases. By convention, when P_j is positive it means that there is a concentric contraction (energy generation) and when it is negative there is an eccentric contraction (energy absorption).[1] In Figure 3.1.3 are represented the hip, knee, and hip joint powers (normalized for cadence and for body weight) for a slow cadence walk from literature and the results obtained in the laboratory session.

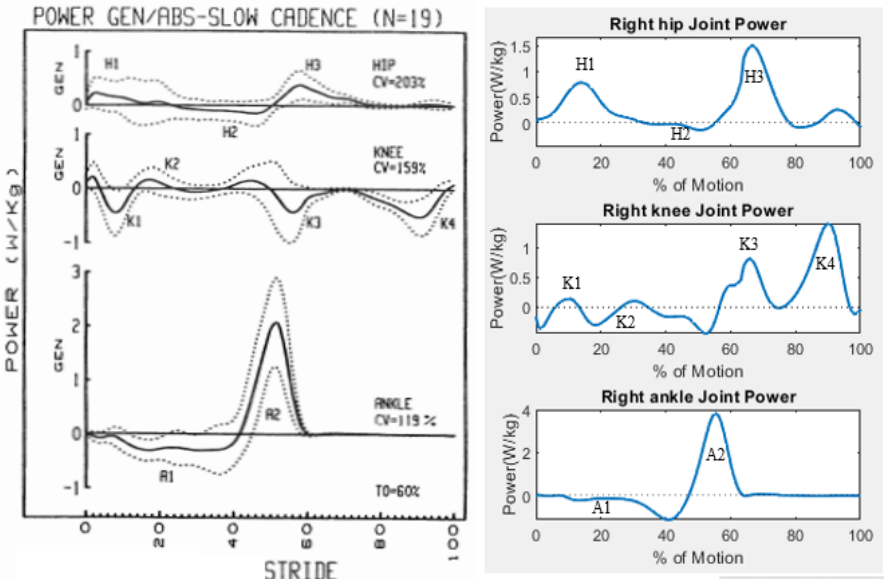

Figure 3.1.3: (From top to bottom) Joint Power of right hip, knee, and ankle joints. Left: Retrieved from literature.[1] Right: Results obtained with the implementation on MATLAB.

In general, the curves obtained relate to the shape of those from literature, when considering the variability across subjects.

For the hip, at initial contact, muscles contract concentrically and generate power (H1). At heel rise there is a small but increasing internal hip flexor moment and, as the hip moves into extension, there is a resulting power absorption (H2). Around opposite initial contact, as the direction of hip motion reverses from extension to flexion, there is power generation (H3).[6] However, hip powers are mainly to maintain trunk balance at slow cadences, being that they can be quite variable between individual strides, especially considering the condition of having to walk on the force plates.[1]

At the knee, it is taken to account that the obtained curve is inverted in relation to its reference, as explained in the previous paper.[3] In opposite toe off, as the knee flexes, there is eccentric muscle contraction and power absorption (K1). During mid-stance, as the direction of knee motion changes from flexion to extension, power generation takes place (K2). During terminal stance, begins flexion of the knee, which causes eccentric contraction

of muscles and results in power absorption (K3). When in terminal swing, there is an eccentric contraction of another muscle, with power absorption associated (K4).[6]

Finally, in the ankle, throughout mid-stance and into terminal stance, there is an increasing internal plantarflexor moment, generated by muscles contracting eccentrically and absorbing power (A1). At opposite initial contact, the plantarflexor moment has increased sufficiently to cause active and rapid plantarflexion of the ankle, promoted by concentric contraction, and resulting in a large generation of power (A2), which is the highest power generation of the entire gait cycle. This power generation is sufficient to accelerate the limb forward into the swing phase.[6]

3.2 Mountain Climber

For the kinetic analysis of the Mountain Climber exercise, it is important to note that it was not possible to compare the obtained results with the literature, since kinetic studies for this movement are scarce.

For each repetition, its start and end regard the event of the left toes touching the ground, being in between the same event for the right toes (red dashed lines in the figures which represent the superimposed repetitions, being excluded the first repetition). The movement started with the hands resting in the plate 3, in an extended plank position, and the feet resting in the plate 1.

3.2.1 Ground Reaction Forces

We obtain the ground reaction forces for both legs (Fig, 3.2.1-A) and both arms (Fig.3.2.1-B) the same way as in the gait analyses, but in this case, we have no literature to compare the results. In these cycles the motion starts with the left leg on the plate, and the red dashed vertical line represents when the right leg reaches the plate.

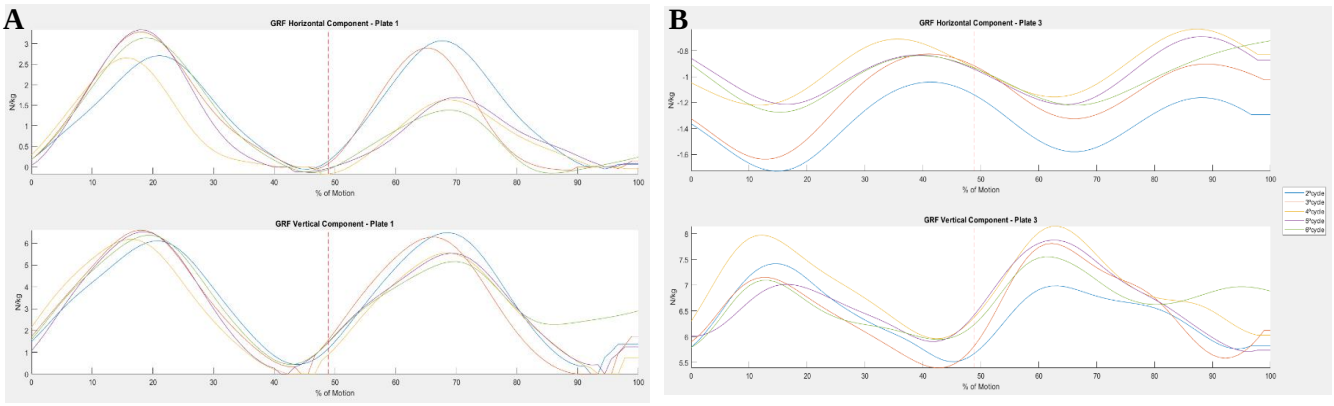

Figure 3.2.1: Horizontal (Top) and vertical (Bottom) Ground Reaction Forces, regarding plate 1, and plate 3 (A- for both legs and B- for both arms).

For the GRF of both legs, we observe some oscillation between the cycles for the horizontal component, which relates to the acceleration and deceleration of the legs, which on the right leg decreased as the analyses proceeded. It is expected a higher value on this component as the speed of the movement increases.

Regarding the GRF of both arms, we observe a big oscillation on the vertical component, synced with the GRF of both legs. This can be explained as a reaction to keep the upper body still, while the legs accelerate.

3.2.2 Moment of Force

To evaluate the net result of the forces resulting in angular rotational of the joints, the moment of force, performed in this movement, we will study the moment of force in the lower body, represented in figure 3.2.2, normalized for body weight.

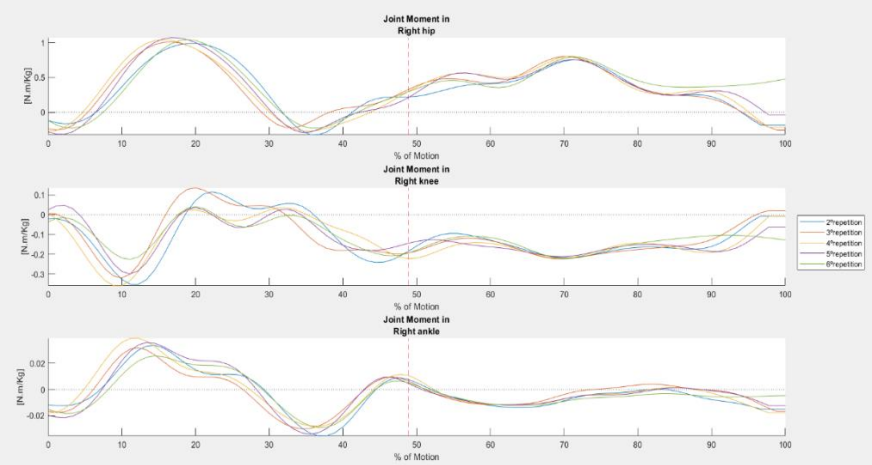

Figure 3.2.2: (From top to bottom) Moment of force for right hip, knee, and ankle joints.

In Figure 3.2.2, we observe that the first half of the cycle starts with a flexor moment in the hip and knee, that results in the flexion of both joints, and then an extensor moment, weaker than the previous moment, that results in the extension of both joints.

As the right foot touches the ground, there is a flexor moment in the hip and knee, that is prolonged for the rest of the cycle, to avoid the collapse of the plank do to the lower body.

3.2.3 Joint Power

To evaluate the mechanical power of a joint we calculate it using the equation (3.2). In Figure 3.2.3 are represented the hip, knee, and hip powers, normalized for body weight.

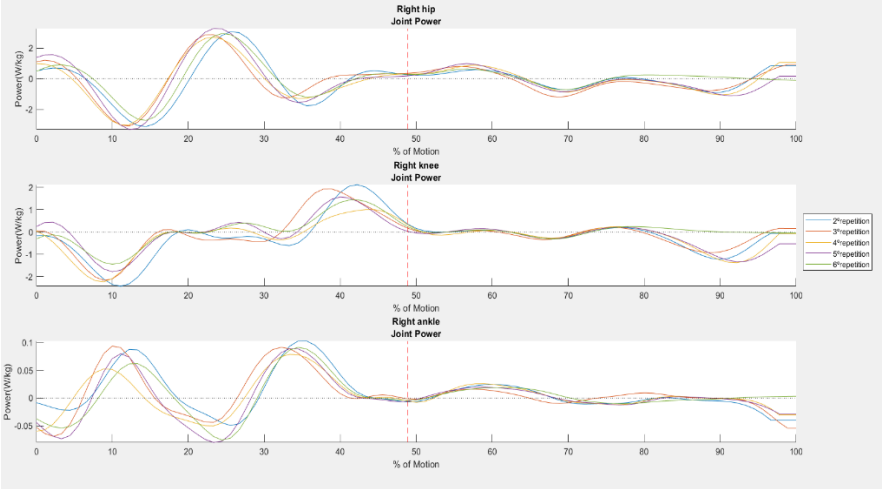

Figure 3.2.3: (From top to bottom) Joint power, right hip, knee, and ankle joints.

In figure 3.2.3 the energy generated as a small peak at the start due to concentric muscle contraction, that is followed by an energy absorption as the joint starts to flex, and then generates energy as it reaches the full flexion of the hip.

Regarding the joint power of the knee, there is a sudden energy absorption right as the knee starts to flex, and then releases it as the knee fully extend, to help dampen the impact of the leg om the floor.

As the right foot touches the ground, we observe that there is almost no power on these 3 joints, since the leg is supposed to be at a standstill.

4 EMG data

The EMG is considering the single best representation of the neurological control (activation) of skeletal muscle. For the recording of EMG involving surface electrodes, provides a less specific measurement, due to the interference from adjacent muscles (phenomenon of "cross-talk"), movements artefacts or electromagnetic interference.[1][6]

Regarding the analysis of the EMG data, it has been reported that the amplitude and shape of unprocessed (raw) EMG data is difficult to interpret, not allowing to quantify their stride-to-stride variability. For improving the assessment, EMG profiles can be obtained by linear envelope processing (full wave rectifier followed by a low pass filter). The EMG linear envelope profiles can be further normalized to the mean of the EMG signal in microvolts (μV) as 100%, to account for intersubject variability.[1] It is important to note that the processing technique employed on the EMG data provided was the RMS envelope, although also being a rectifying and smoothing technique.

4.1 Gait movement

In order to have a full understanding of the normal gait, it is necessary to know which muscles are active during the different parts of the gait cycle.

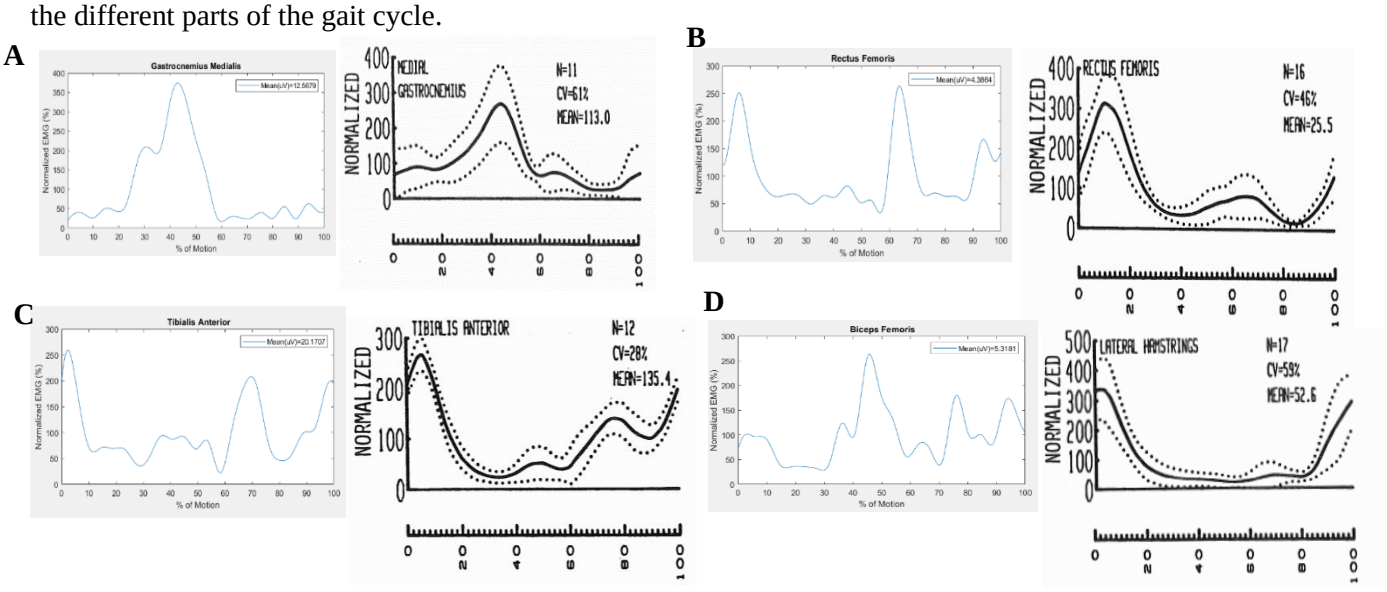

Figure 4.1: Representation of EMG plots regarding the 4 assessed muscles, while performing the gait movement. A) Gastrocnemius Medialis (GM). B) Rectus Femoris (RF). C) Tibialis Anterior (TA). D) Biceps Femoris (BF). (Left) Data obtained from the lab. (Right) Results expressed in the literature (Winter [1]).

Regarding the GM muscle, the maximal peak of activity is consistent with the revised literature, occurring approximately at 40% of the stride, during the stance phase, corresponding to the shortening of the muscle to cause

the foot to actively plantar flex during lift off. After the maximal peak, the activity drops rapidly, being kept at a low level until the end of the swing phase, being the observed validated by the literature [1]. The disturbance in the EMG activity before the mentioned peak could be due to the subject's gait being conditioned to the 3 force plates positioned on the floor, which could explain a possible hesitation when lifting the right heel.

For the RF muscle, its major activity is reported in the beginning of the gait, related to the right heel contact with the ground during weight acceptance (10% stride), when it acts as a knee extensor to control knee flexion and causes the knee to extend in mid stance [1]. This peak was observed, although being approximately at 5% of the stride. Besides this peak, a minor burst of activity (close to 65%) is also reported by the literature, related to the hip flexion, pulling the swinging limb forward, and knee extension, decelerating the backward swinging leg and foot [1]. In fact, this peak was observed in the collected data, although having a similar amplitude to the first one.

Regarding the TA muscle, its major activation is reported as generating forces to lower the foot to the ground, corresponding to controlled plantar flexion at the ankle [1], being the data acquired concordant with the literature. A second burst of activity is approximately predicted at 50% of the stride, being associated to the toes lifting off, promoting dorsiflexion of the foot for foot clearance during mid swing. At approximately 70% of the stride, the predicted peak by the literature was reproduced, being related to pulling the leg forward over the foot.[1]

Finally, the BF is described as a long muscle of the posterior side of the thigh, being commonly called hamstrings when considering it together with the semitendinosus and semimembranosus muscles. Comparing with the other EMG profiles analyzed, the activation of the BF is more irregular. From the literature, the major peaks occur in the extremities (beginning and end of the stride), related to the muscle acting as hip extensor, during weight acceptance, and in the deceleration of the leg [1]. However, from the obtained results, besides having more oscillations in the muscle activation, the major peak is almost centered (45% of the stride).

Overall, the differences in the results obtained from the ones found in the literature can be explained by the following factors: different processing techniques employed on the raw EMG data; only one isolated gait cycle was assessed for the data collected, not allowing to account for intra-subject variability; inter-subject variability; the subject's gait was conditioned to the 3 force plates positioned on the floor; redundancy in muscle activity, being possible to achieve the same movement, as measured kinematically, from a score of different combinations of muscle patterns, as many of the muscles involved on walking have a synergistic and antagonistic nature.[1] [6] It is also important to mentioned that the relationship between force of contraction and EMG activity is far from straightforward.[1]

5 Conclusion

The present work relied on the implementation and detailed study of the dynamic analysis regarding a pre-defined 2D multibody system considering the data acquired in the laboratory when a supposedly healthy subject had performed the gait and the mountain climber exercise.

Regarding the gait cycle, the results obtained are mostly in accordance with the revised literature, validating the constructed 2D model as well as the computational implementation developed. The computational methods applied could also explain the observed differences, such as the filtering process and the multibody model chosen and the differences in the amplitudes registered resulting of the normalization process. However, the overall enveloping configurations of the experimental EMG curves for the gait cycle resemble the ones in the literature.

In the implementation of our code the intersubject variability was taken into account to a better comparison when cross-validating results with the literature.

As for the mountain climber movement, the comparison with references was not possible, due to the lack of dynamic studies regarding this motion. Nevertheless, the acquisition analyzed was enough to understand the dynamics of the system, and results explained well the movement, without anything to emphasize.

References

[1] David A. Winter, The Biomechanics and Motor Control of Human Gait. Waterloo, Ontario, Canada: University of Waterloo Press, 2 ed, 1988.

[2] Susan J. Hall, Basic Biomechanics, pp. 2-3. 2 Penn Plaza, New York: McGraw-Hill Education, 7 ed, 2015

[3] A. Lopes, D. Galhoz, M. Mourão and R. Almeida, "Kinematic Analysis of Human Movement: Gait and Mountain Climber", Instituto Superior Técnico, Universidade de Lisboa, 2020.

[4] IST Integrated Master's in Biomedical Engineering, "Biomechanics of Human Motion 2020-2021 - week 08", 2020

[5] IST Integrated Master's in Biomedical Engineering, "Biomechanics of Human Motion 2020-2021 - week 09", 2020

[6] Michael W. Whittle, Gait Analysis: An Introduction, pp. 52-80. Oxford: Butterworth-Heinemann Ltd., 4 ed, 2007.

[7] IST Integrated Master's in Biomedical Engineering, "Biomechanics of Human Motion 2020-2021 - week 07 (Practical)", 2020.

Appendix A

Table A.1: Structure considered for the input file of the 2D biomechanical multibody, DraftBiomechanicalModel.txt, read by the function ReadProcessingFile.m. Values for the mass, radius of gyration, position of the center of mass (PCoM), ζ/L and η/L accessed from [7].

NBodies	**NRevolute**		**NGround**		**NDriver**		**NFplates**
Body (1,…,14)	Prox. Point, *pi*		Dist. Point, *pj*		PCoM	Mass	Radius of Gyration
Rev. J. (1,…,13)	Prox. Body, *i*	Dist. Body, *j*	ζ_i/L_i	η_i/L_i	ζ_j/L_j	η_j/L_j	-
Driver (1,…,16)	Type	Prox. Body, *i*	$Coord_i$	Dist. Body, *j*	$Coord_j$	filename	-
Force Pl. (1,2,3)	Prox. Body, *i*	Dist. Body, *j*	ζ_i/L_i	η_i/L_i	ζ_j/L_j	η_j/L_j	filename

Appendix B

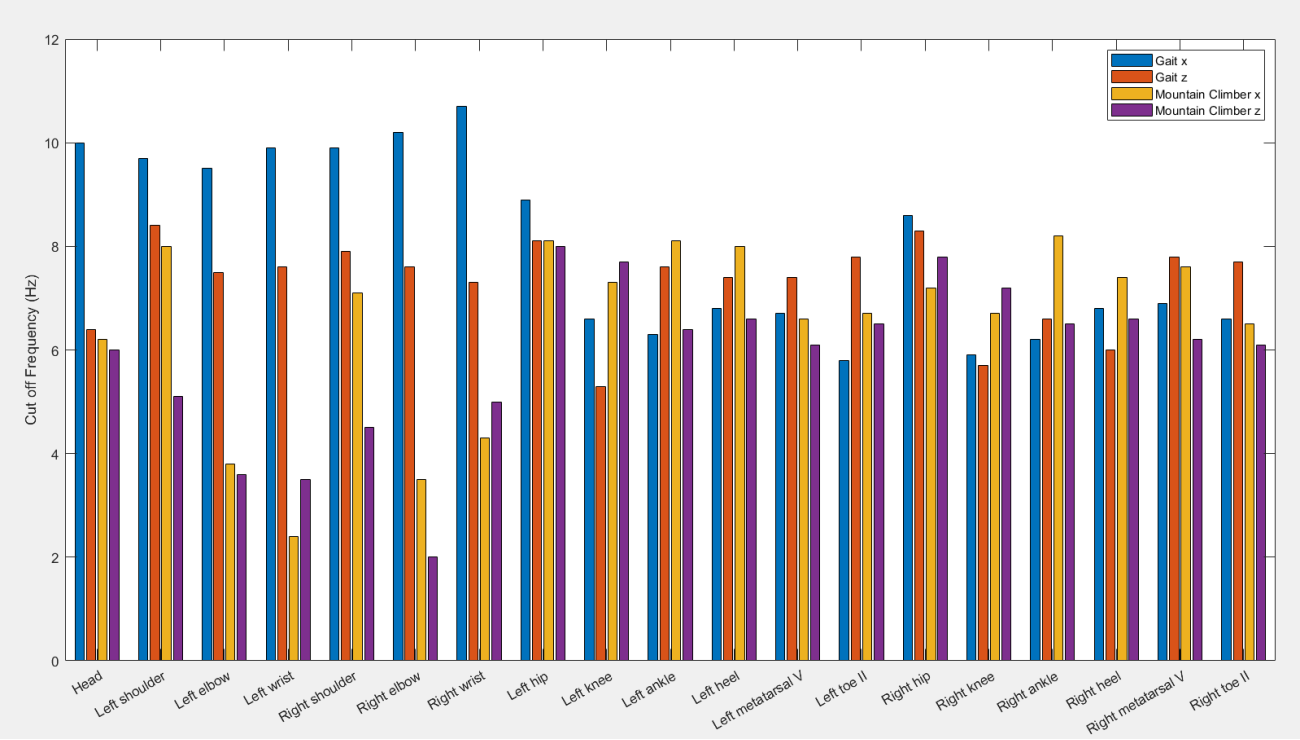

Figure B.1: Cut-off frequencies obtained through residual analysis, used for low-pass filtering the position data regarding each body, for the gait and mountain climber movements.

Appendix C

Table C.1: Cycles_MountainClimber.txt file, which organizes relevant information for determining the periods of each repetition of the mountain climber movement acquired. The first line contains the initial frame (nframe_initial) at which the dynamic movement acquisition started, as well as the number of repetitions (num_cycles). The next two lines contain the previously mentioned frames of first contact with the floor for right and left toes, respectively. It is important to note that the EMG data was acquired with a sampling frequency of 1000 Hz, whereas the kinematic and kinetic data provided have a sampling frequency of 100 Hz. Thus, the previous obtained indexes were transformed in order to access the same time instants, having been confirmed that this was successfully done.

1	nframe_initial	num_cycles				
2	nr_1	nr_2	nr_3	nr_4	nr_5	nr_6
3	nl_1	nl_2	nl_3	nl_4	nl_5	nl_6